Archaeological Prospection
Archaeol. Prospect. **20**, 39–44 (2013)
Published online 13 February 2013 in Wiley Online Library
(wileyonlinelibrary.com) DOI: 10.1002/arp.1437

Short Report

An Interdisciplinary Non-invasive Approach to Landscape Archaeology of the Great War

TIMOTHY SAEY[1]*, BIRGER STICHELBAUT[2], JEAN BOURGEOIS[2], VEERLE VAN EETVELDE[3] AND MARC VAN MEIRVENNE[1]

[1] *Research Group Soil Spatial Inventory Techniques, Faculty of Bioscience Engineering, Ghent University, Coupure 653, 9000 Gent, Belgium*
[2] *Department of Archaeology, Faculty of Arts and Philosophy, Ghent University, Sint-Pietersnieuwstraat 35, 9000 Gent, Belgium*
[3] *Department of Geography, Faculty of Sciences, Ghent University, Krijgslaan 281 S8, 9000 Gent, Belgium*

ABSTRACT The prospection and evaluation of former battlefields of the Great War or the First World War (WW I) poses specific challenges. For several reasons, large-scale excavation campaigns of this conflict landscape are problematic. The vastness of the former Western Front (one of the largest archaeological sites in the world), the large amounts of buried unexploded ordnance and the possible presence of human remains hinder invasive practices. As an alternative, an integrated approach combining a geophysical survey, contemporary aerial photographs and a topographic model is proposed. This approach was evaluated for a 3.2 ha WW I battlefield using a multireceiver electromagnetic induction (EMI) sensor. Integrating multiple apparent electrical conductivity (ECa) and apparent magnetic susceptibility (MSa) EMI measurements allowed evaluation of the present WW I remains in the subsoil, while comparison with WW I aerial photographs and a digital terrain model led to a comprehensive understanding of the WW I landscape. It is suggested that this approach may be of value for the investigation of battlefields in other locations and periods. Copyright © 2013 John Wiley & Sons, Ltd.

Key words: Conflict archaeology; World War I; electromagnetic induction; aerial photography; digital terrain model

Introduction

The approaching centennial of the onset of the Great War, or the First World War (WW I), in 2014 has triggered a renewed interest in the history and memory of this violent episode in European history. During WW I, for the first time, aerial photography rapidly developed as an intelligence tool that saw large-scale application by both sides (Grand Quartier Général des Armées, 1916; Kommandierender General der Luftstreitkräfte, 1917). From the end of 1915 onwards, photoreconnaissance units were sent out on a regular basis along the Western Front to record the outline of the enemy's defences (Carlier, 1921). Large numbers of these photographs have survived in archives all over Europe, the USA and Australia. These are a primary record of the progress of WW I, and are also a valuable source of data for landscape researchers in general, landscape archaeologists and cultural resource managers (Chielens *et al.*, 2006; Decoodt, 2007). Moreover, they allow an understanding of the structure and evolution of the conflict landscape during WW I and aid investigation of the original composition of the heritage (Stichelbaut, 2011; Gheyle *et al.*, 2013). Nowadays, questions about the presence, nature and diversity of the WW I relics as well as their context in the landscape are raised. Some of the features, for example mine craters and bunkers, are still visible in the current landscape, although the majority of the surviving features are preserved beneath the surface.

* Correspondence to: T. Saey, Research Group Soil Spatial Inventory Techniques, Faculty of Bioscience Engineering, Ghent University, Coupure 653, 9000 Gent, Belgium. E-mail: timothy.saey@ugent.be

Received 20 December 2012
Accepted 7 January 2013

After the war, the former battlefields were largely cleared above ground, but the subsurface war traces became part of the archaeological soil archive.

At former battlefields, invasive practices for characterizing the archaeological heritage are hampered by the possible presence of human remains and unexploded ordnance. As an alternative, geophysical prospection has been selected as a useful tool to non-invasively map buried relicts of WW I battlefields (Masters and Stichelbaut, 2009; Saey *et al*., 2011), due to their success in locating metallic and non-metallic artefacts. Magnetometer prospecting represents one of the widest employed tools in geophysical research applied to archaeological studies, and therefore also for conflict archaeological surveys (Bossuet *et al*., 2001). However, Masters and Stichelbaut (2009) recorded magnetic noise attributable to shrapnel dispersed in the topsoil, thus making underlying WW I features indistinguishable. A fluxgate gradiometer survey from Sutherland and Schmidt (2003) showed that modern anomalies obscure potential medieval artefacts and that magnetometer surveys are therefore not suited for mapping archaeological features in the presence of strongly disturbing overlying features.

The advantage of using electromagnetic induction (EMI) is the ability for mapping the subsoil archaeological structures where the topsoil has been disturbed. The EMI instruments measure simultaneously the soil apparent electrical conductivity (ECa) and apparent magnetic susceptibility (MSa) (Simpson *et al*., 2009). Measurements of the MSa exhibit similar anomalies due to magnetic susceptible materials such as gradiometers. Moreover, the simultaneous measurement of ECa allows the identification of small features, contrasting with the surrounding soil due to different soil physical properties (Carroll and Oliver, 2005). Furthermore, both ECa and MSa signals have the ability to detect metallic objects. By using a multireceiver EMI, multiple ECa and MSa measurements from different soil volumes can be obtained simultaneously (Saey *et al*., 2009; Sudduth *et al*., 2013). Combining these measurements enables extracting depth information about the archaeological features (Saey *et al*., 2012). So, the integration of the simultaneous measurements has the potential to improve both the vertical and horizontal discrimination of magnetic and conductive features.

In this study, we propose a novel combination of non-destructive technologies for mapping the conflict landscape of WW I, including the deployment of a multireceiver EMI soil sensor, the processing of WW I aerial photographs and a digital terrain model. A landscape archaeological analysis is required to comprehend the complex interaction between the human activities and the physical environment and understand the link between the war activities and the landscape in which they took place. Therefore, the objective is to develop an interdisciplinary methodological approach for assessing the present-day buried remains of the WW I conflict landscape. The study area of 3.2 ha (central coordinates: 50°47′17"N and 2°47′26"E) is located near Ypres (Belgium) at the foot of Mount Kemmel (Kemmelberg) (Figure 1).

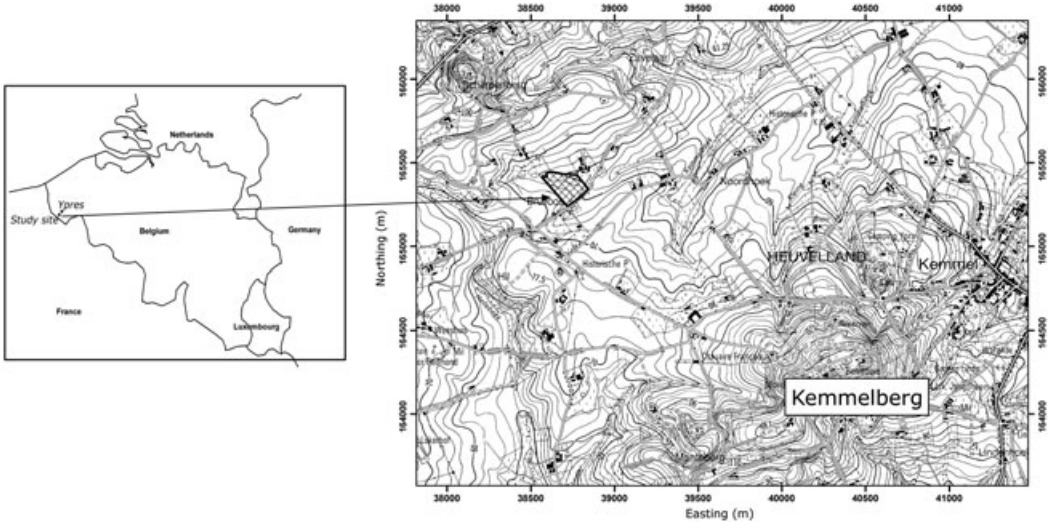

Figure 1. Location of the study site in Belgium and topographic map of the area of the study site (black).

DOI: 10.1002/arp

Aerial photographic interpretation

For the study area, 24 different aerial photographs were available, dating from 18 April 1915 to 17 July 1918 and covering different phases of the war in the Ypres Salient. The German and Allied aerial photographs originate from the Bayerisches Hauptstaatsarchiv in Munich, the Belgian Army Museum in Brussels and the Imperial War Museum in London (Stichelbaut, 2011).

Within the study area, the first war activities were situated in the northwestern corner between 18 April 1915 and 9 July 1916, and were interpreted as a series of shelters (Figure 2). One of the shelters evolved into a small pond. An aerial photograph of 25 May 1917 depicts a military road, which passed straight through the site, connecting a military barrack in the west with 'Butterfly Camp', 400 m to the east. On 25 April 1918 the German forces launched an attack on Mount Kemmel, which was defended by French troops. The hill was the theatre of fierce fighting before the Germans succeeded in capturing the hill and advancing towards the site, which became part of the frontline. During that period, the site was bombed heavily, as witnessed by the numerous shell holes visible on the aerial photograph from 3 May 1918. Between 3 May and 7 May 1918, an Allied (French) trench was constructed in the middle of the surveyed area (Figure 2a). Because the activity traces (visible as the white band adjacent to the trench on Figure 2a) are on the northern side of the trench, it has been constructed as a defensive trench against an attack from the south. This trench is by no means a heavily constructed fire trench, its trace being irregular and in some places discontinuous. The last available aerial photograph, from 17 July 1918 (Figure 2a), shows two large shelters in the vicinity of the trench, which was at that time the third line of defence.

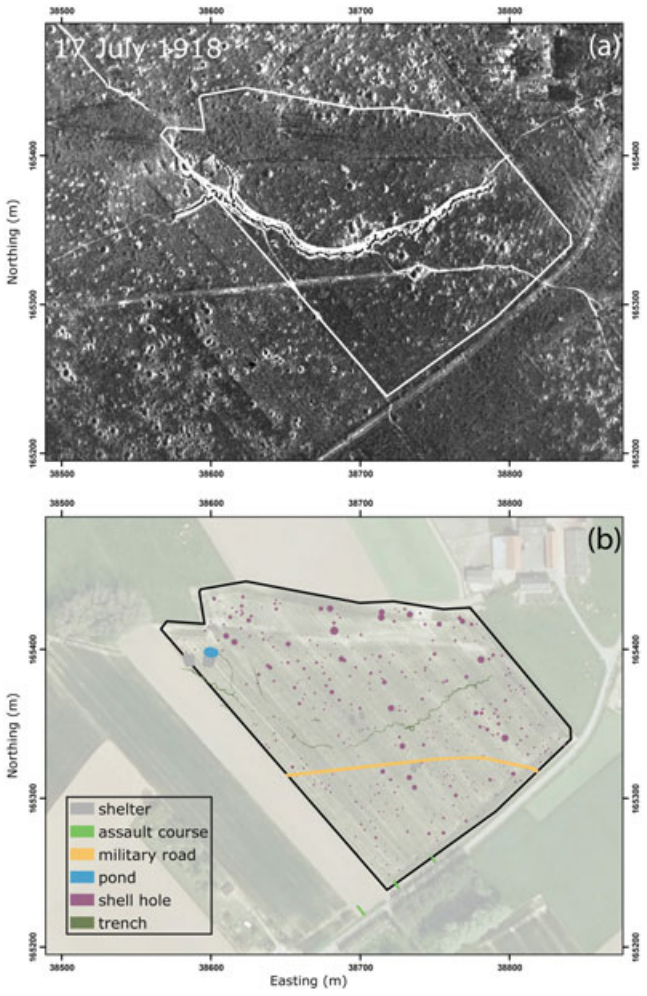

Figure 2. (a) Aerial photograph of the study site on 17 June 1918 (top) and (b) interpretation of the features digitized from a sequence of 24 photographs taken during WW I (bottom). This figure is available in colour online at wileyonlinelibrary.com/journal/arp

The EMI survey

On the study site, the ECa and MSa was investigated with the DUALEM-21S EMI soil sensor, pulled behind an all-terrain vehicle at a speed of about 6–10 km h^{-1}, crossing the field at parallel lines 0.85 m apart. Within lines, measurement intervals were at about 0.2 m. The eight simultaneous ECa and MSa measurements and differential global positioning system (DGPS) coordinates were recorded by a field computer. The DUALEM-21S instrument (DUALEM, Milton, Canada), consisting of one transmitter coil and four receiver coils, was located at distances of 1, 1.1, 2 and 2.1 m. The 1 and 2 m transmitter–receiver pairs form a vertical dipole mode (1HCP and 2HCP), while the 1.1 and 2.1 m pairs form a perpendicular dipole mode (1PRP and 2PRP) (Saey *et al.*, 2009). The MSa measurements in the PRP coil configurations are generally very noisy and less useful compared with both measurements in HCP mode.

Table 1 shows the summary statistics of the 6 × 138 291 ECa and MSa measurements taken with the DUALEM-21S sensor. The mean values of the ECa in the

Table 1. Descriptive statistics (*m*, mean; *s*, standard deviation) of the ECa and MSa measurements ($n = 138\ 291$).

Variable	Configuration	*m*	Minimum	Maximum	*s*
ECa (mS m^{-1})	1PRP	18	−95	159	6
	2PRP	25	−40	70	5
	1HCP	25	−17	89	6
	2HCP	35	−1	70	5
MSa (10^{-4} msu SI)	1HCP	12	−48	65	1.8
	2HCP	36	−285	71	4.6

DOI: 10.1002/arp

2PRP and 1HCP coil configurations are almost identical, larger than the shallower ECa of the 1PRP coil configuration and smaller than the deeper ECa of the 2HCP coil configuration. This indicates that, on average, the topsoil is less conductive than the subsoil up to 1.5 m, and this subsoil is on its part less conductive compared with the soil volume deeper than 1.5 m. The strong negative minimum values for all coil configurations and the same very high maximum values are caused by metal anomalies buried in the soil. The standard deviations are similar for the four ECa measurements. The MSa measurements with the HCP coil configuration are less straightforward to interpret, but the measurements obtained with the 1 m coil spacing are on average lower and less variable than those measured with the 2 m coil spacing.

Figure 3 shows two of the four ECa measurements, interpolated with ordinary kriging to a 0.1 m by 0.1 m grid. In particular the ECa measurements in the 1PRP (Figure 3a) and 2HCP (Figure 3b) coil configurations depict the main trench within the study area as a sequence of anomalies. Metal objects in the subsoil cause positive ECa peaks in the 1PRP configuration and negative ECa anomalies in the 2HCP configuration. This inverse pattern for both configurations can be attributed to the presence of buried metal objects in the soil (Saey *et al*., 2011). On this study site, the MSa map in the 2HCP configuration (Figure 3c) depicts largely similar patterns and anomalies compared with the ECa maps. Features appearing on both the ECa and MSa maps are caused by buried metal objects in the soil, and features appearing only on the MSa maps are due to magnetized material (e.g. fire places and brick material). The study site was heavily affected by shell impacts, which left their mark in the soil and can be seen as both magnetic and conductive anomalies across the entire area surveyed. Due to its specific depth response, the 2HCP coil configuration is predominantly effected by features present in the top 1 m of the soil. A large similarity was observed between the features digitized from all aerial photographs (Figure 2b) and the magnetic anomalies on the MSa map of the 2HCP coil configuration. Because this coil configuration amplifies the anomalies caused by deeply buried shells while suppressing the anomalies from shallow shrapnel and other metal remains, most impacts were considered relatively deep. The Allied trench can be observed as a rectilinear magnetic anomaly running across the study site (A on

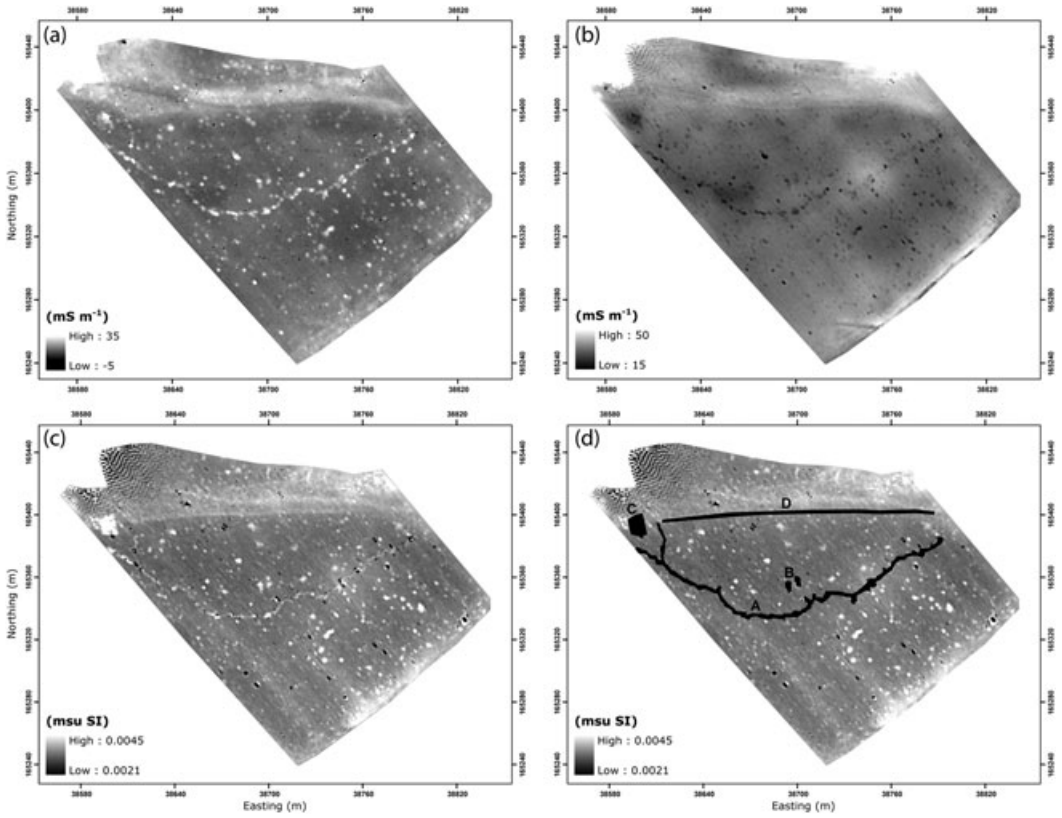

Figure 3. (a) Apparent electrical conductivity (ECa) measurements of the 1PRP coil configuration; (b) of the 2HCP coil configuration (in mS m^{-1}); (c) apparent magnetic susceptibility (MSa) measurements of the 2HCP coil configuration (in msu SI); and (d) identification of the features discussed in the text.

DOI: 10.1002/arp

Figure 3d). The trenches were reinforced and lined with corrugated iron sheets, which aids in the detection of such features. Compared with the ECa maps, the trench could be delineated sharper from the MSa map. Just behind this trench, it is possible to identify the two large shelters (B on Figure 3d) that appear on the aerial photograph of 17 July 1918 (Figure 2a). Moreover, only the MSa map revealed both the large shelter in the northwest of the study site, which was later transformed a pond (C on Figure 3d), and a linear feature crossing the study site from west to east (D on Figure 3d).

Integrated visualization

To remove the influence of natural soil variability on the measurements and focus on the local anomalies in the data, a filtering procedure was applied. The extreme values were converted to the mean value of the neighbouring measurement points within a circular search area with a radius of 10 m. The gradual natural trend was subtracted from the original ECa measurements to obtain the ΔECa for each particular coil configuration. After obtaining the ΔECa values, these were optimally combined to the 'fused electromagnetic metal prediction (FEMP)' as

$$FEMP = 2.05\ \Delta ECa_{1PRP} - \Delta ECa_{2PRP} - 0.82\ \Delta ECa_{1HCP} - 1.89\ \Delta ECa_{2HCP}$$

with ΔECa_{sC} the ΔECa for coil spacing s and coil configuration C (Saey *et al.*, 2011). The map obtained represents an integration of the four ΔECa maps with the aim of delineating buried metal objects. On this map, positive anomalies represent metal objects down to 1.0 m, while negative FEMP values predict the absence of metal objects in the soil profile. It was draped on a three-dimensional representation of the soil surface elevation, which was recorded with our DGPS (Figure 4). When comparing the aerial photograph taken on 7 May 1918 (Figure 4a) with the FEMP map (Figure 4b), a strong similarity is observed between the present buried remains of the WW I infrastructure and the features visible during the conflict. The identification of a structured buried metal response suggests that the site was not thoroughly cleaned up after WW I. The correspondence between both aerial photograph and FEMP map proved the potential of EMI for identifying the remains of a battlefield. The trench system, shellholes and metal fragments are easily recognized from this map. However, some metal objects did not show on the aerial photographs. These could represent unexploded shells, metal remains from shells exploded after 17 July 1918, or more recent metal-containing material

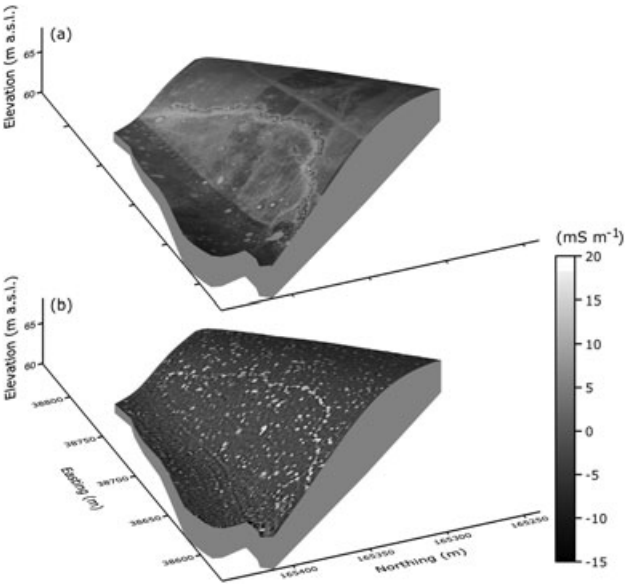

Figure 4. (a) Current topography draped with the aerial photograph of 7 May 1918; (b) current topography draped with FEMP map, indicating the presence of buried metallic objects.

buried in the subsoil. On the other hand, both ECa and MSa measurements could not identify the military road crossing the study area and two associated shelters. Presumably this non-identification is due to the absence of electromagnetically contrasting material in the features.

The integrated representation shown in Figure 4 aids the interpretation of the WW I features in the surrounding landscape. This allows a better understanding of the spatial relationship between the WW I features and the landscape; this relationship helps to account for the military actions undertaken. The position of the WW I features was largely influenced by the presence of the east–west running ridge on which the study site is situated. The WW I features were located in the vicinity of this ridge because of strategic advantages. Based on the three-dimensional representation, it can be stated that the trench was predominantly located just behind the uppermost part of the ridge. For strategic reasons, ridges and upslope areas were preferred over lower lying areas. The upslope position in the landscape was chosen for a better defence of the soldiers against the enemy and therefore was crucial in choosing the location of the trench. Moreover, locating the trench just behind the uppermost part of the ridge gave the Allied forces a natural protection by the landscape. It was buil into the slope, with limited visibility for the German forces present at the other (southern) side of the ridge. Moreover, this trench system bended and branched off to the northern, lower lying part of the study site. Probably, this allowed the soldiers to escape to safer areas in times of heavy artillery fire.

DOI: 10.1002/arp

The integrated analysis of the available information enabled an enhanced assessment of the WW I conflict landscape. The complex interaction between the human activities and the physical environment was gathered by the interdisciplinary, landscape archaeological approach, which can support the evaluation and future management of the WW I heritage.

Conclusions

The interdisciplinary approach, integrating multiple simultaneous signals from a multireceiver EMI instrument, a time sequence of wartime aerial photographs and a digital terrain model, allowed a detailed, non-invasive inventory of WW I battlefield remains in their surrounding landscape. By adding an aerial photographic approach to the geophysical prospection, insight into the typology, origin and diversity of war features was obtained. Such a situation, where the remote sensing data is contemporary with the archaeological remains, is highly unusual. The EMI survey identified the current remains at a WW I battlefield, allowing the location of structures that had been buried or only temporarily erected and consequently missed by aerial photography, while geophysical measurements were unable to detect without a substantial electrical or magnetic contrast in the soil. The integration of geophysics, aerial photography and topography allowed a three-dimansional visualization of the WW I structures in the landscape, which contributed to an enhanced understanding of the historical reality during the First World War. This study suggests that a more frequent use of this interdisciplinary approach in prospecting sites that were battlefields in different periods may be profitable.

Acknowledgements

The EMI survey was funded by the province of West Flanders. The authors would like to thank Marc Dewilde for providing us details of the WW I study site, Valentijn Van Parys for his assistance with the field work and the farmer Bernard Deconinck for granting us access to his field.

References

Bossuet G, Camerlynck C, Brehonnet C, Petit C. 2001. Magnetic prospecting of diachronic structures (antiquity to First World War) on the site of the sanctuary of Ribemont-sur-Ancre (Somme, France). *Archaeological Prospection* **8**: 67–77.

Carlier A. 1921. *La Photographie Aerienne pendant la Guerre*. Librairie Delagrave: Paris.

Carroll ZL, Oliver MA. 2005. Exploring the spatial relations between soil physical properties and apparent electrical conductivity. *Geoderma* **128**: 354–374.

Chielens P, Dendooven D, Decoodt H. 2006. *De Laatste Getuige. Het oorlogslandschap van de Westhoek*. Lannoo: Tielt; 256 pp.

Decoodt H. 2007. De Sporen van 'Den Grooten Oorlog'. *Monument, Landschappen en Archeologie* **26**: 4–36.

Gheyle W, Dossche D, Bourgeois J, Stichelbaut B, Van Eetvelde V. 2013. Integrating archaeology and landscape analysis for the cultural heritage management of a World War One militarised landscape. The German field defences in Antwerp. *Landscape Research* DOI: 10.1080/01426397.2012.754854.

Grand Quartier Général des Armées. 1916. Notes sur l'Interprétation des Photographies Aériennes. S.l., s.n.

Kommandierender General der Luftstreitkräfte. 1917. Bildmeldung der Luftschiffer. Charleville, s.n.

Masters P, Stichelbaut B. 2009. From the air to beneath the soil – revealing and mapping great war trenches at Ploegsteert (Comines-Warneton), Belgium. *Archaeological Prospection* **16**: 279–285.

Saey T, Simpson D, Vermeersch H, Cockx L, Van Meirvenne M. 2009. Comparing the EM38DD and DUALEM-21S sensors for depth-to-clay mapping. *Soil Science Society of America Journal* **73**: 7–12.

Saey T, Van Meirvenne M, Dewilde M, *et al*. 2011. Combining multiple signals of an electromagnetic induction sensor to prospect land for metal objects. *Near Surface Geophysics* **9**: 309–317.

Saey T, De Smedt P, Meerschman E, *et al*. 2012. Electrical conductivity depth modelling with a multireceiver EMI sensor for prospecting archaeological features. *Archaeological Prospection* **19**: 21–30.

Simpson D, Van Meirvenne M, Saey T, *et al*. 2009. Evaluating the multiple coil configurations of the EM38DD and DUALEM-21S sensors to detect archaeological anomalies. *Archaeological Prospection* **16**: 91–102.

Stichelbaut B. 2011. The first thirty kilometres of the western front 1914–1918: an aerial archaeological approach with historical remote sensing data. *Archaeological Prospection* **18**: 57–66.

Sudduth KA, Myers DB, Kitchen NR, Drummond ST. 2013. Modeling soil electrical conductivity–depth relationships with data from proximal and penetrating EC_a sensors. *Geoderma* DOI: 10.1016/j.geoderma.2012.10.006.

Sutherland T, Schmidt A. 2003. Towton, 1461: An integrated approach to battlefield archaeology. *Landscapes* **4**: 15–25.